doi: 10.56761/EFRE2022.C1-P-021302

# Numerical simulation of the features and regularities of the high-power density ion beam formation

*A.I. Ryabchikov*[1,*], *V.P. Tarakanov*[2]

[1]*National Research Tomsk Polytechnic University, Tomsk, Russia*
[2]*National Research Nuclear University MEPhI – Moscow Engineering Physics Institute, Moscow, Russia*
[*]*ralex@tpu.ru*

**Abstract.** The development of methods to modify materials based on the synergy of high-intensity implantation and simultaneous energy exposure is intended at creating deep ion-doped layers. For this purpose, it is proposed to use pulsed and repetitively-pulsed beams of metal and gas ions with micro-submillisecond duration with a high-pulsed power density. The paper presents the results of numerical simulation of the pulsed and repetitively-pulsed high-intensity ion beam formation. Simulations were performed using the Karat code. The ballistic focusing of heavy ions was studied at injection current from 0.1 to 1 A. The influence of the ion current density, accelerating voltage, ion charge composition, and conditions for neutralizing the beam space charge on the high-power ion beam transport and focusing has been studied. The conditions for the virtual anode appearance have been determined and studied. It has been found that for long durations of ion beam formation at low pressures of the residual atmosphere, multiple appearance and disappearance of a virtual anode is possible. The possibility of ballistic formation of ion beams with a pulse density of hundreds of kilowatts per square centimeter is shown.
**Keywords:** numerical simulation, metal ion beam formation, ballistic focusing, high-power density.

## 1. Introduction

Ion implantation is an important tool for surface modification of a wide range of materials for different applications in the fields of basic research and applied technology [1–4]. New methods of high-intensity implantation using low-energy high-power density ion beams demonstrate the possibility of ion doping of materials at depths of tens of micrometers at ion irradiation fluences of $10^{19}$–$10^{21}$ ions/cm$^2$ [5, 6]. The advantages of the low-energy high-intensity ion implantation (LEHI$^3$) method, providing deep ion doping of materials, are leveled in a number of promising applications by heating the entire sample to high temperatures, at which a significant increase in the material grain structure is observed. A study [7] describes a new method aimed at solving this problem. The essence of the method lies in the use for high-intensity implantation of ion beams with micro-submillisecond duration with a power density from tens to several hundreds of kilowatts per square centimeter. Repetitively-pulsed implantation using such ion beams can provide pulsed heating of a local area near the surface, followed by rapid heat transfer into the target material.

This article focuses on numerical simulation of submillisecond high-power pulsed metal ion beam formation using vacuum arc plasma.

## 2. Numerical simulation of the high-density ion beam formation under conditions of ballistic focusing

For a detailed understanding of all processes and the construction of a holistic model for the formation of submillisecond ion beams with a pulse power density of tens and hundreds of kilowatts per square centimeter, a set of studies was carried out using numerical simulation using the KARAT code [8], in which Maxwell's equations are solved, and the current density is calculated by the large particle method – PIC method. A plasma-immersion formation system was studied, which was experimentally tested for the first time to obtain ballistic-focused repetitively-pulsed metal ion beams with a current density of up to 1 A/cm$^2$ at bias potential amplitudes of up to 3 kV [9]. One of the features of the vacuum arc plasma is associated with the presence of a significant initial energy of directional motion in ions. During the numerical simulation, the plasma flow was simulated by the ion flow with a given current and, accordingly, with a given current

density. The initial energy of directed ion motion was set equal to 50 eV. Simultaneously with the ions, an electron flow was launched, the speed of which corresponded to the ions' speed. In this way, a charge-neutralized particle flow was injected. When the particles approach the electrode, to which the bias potential of negative polarity is applied, the electron flow is retarded, and the ions are accelerated in the sheath that is formed. The flow of accelerated ions penetrates into the drift equipotential space through the grid electrode. The shape of the grid electrode in the form of a part of a sphere with a radius $R$ provides the initial ballistic focusing of ions. To ensure the neutralization of the ion beam's space charge in numerical simulation, several approaches were used. In most cases, plasma with different initial concentrations was created in the beam drift space. In addition, this article studies the influence of ion-electron emission from the irradiated target surface, ionization of the residual gas and additional electron flow on the neutralization of the beam space charge and its transport.

The presence of an ion extractor with a grid structure significantly complicates the numerical simulation process. At the same time, since transport and focusing of an ion beam with an initial density not exceeding 10 mA/cm$^2$ are simulated, at accelerating voltages from 10 to 40 kV, the width of the sheath layer (accelerating gap) is many times greater than the characteristic size of the grid electrode cells. This means that the fine structure of the network will have little effect on the individual ion trajectories. A significant influence of the grid is associated with its transparency, on which the ion beam losses on the grid electrode elements depend. In simulation, the current passing through the grid electrode is considered as the ion injection current. To simulate the conditions for excluding the direct passage of vacuum arc plasma microparticles from the cathode surface to the ion beam focusing region, the central region of the extracting electrode was opaque for ions.

## 3. Simulation of ion beam transport in the absence of its space charge neutralization

Initially, the authors studied ion beam transport and focusing during its injection into the drift space in the absence of conditions for neutralizing its space charge. When an ion beam is injected with a current of 0.01 A, which corresponds to an initial current density of $4 \cdot 10^{-4}$ A/cm$^2$, even in the case when the ion energy is only 10 keV, the ion beam is well focused, although due to the space charge effect, the beam profile in the focal region turns out to be blurry. Along the beam axis, the ion current density at the focus increases to 0.035 A/cm$^2$, i.e. it increases by about 87 times. The increase in the ion energy to 40 keV decreases the ion density due to an increase in their velocity. As a result, the space charge effect decreases and the conditions for beam focusing improve. This improves focusing and the ion current density exceeds to 0.06 A/cm$^2$, which corresponds to an increase in the ion current density compared to the injection current density by almost 400 times. However, the power density of such a beam does not exceed 2.5 kW/cm$^2$, which does not provide the possibility of realizing the synergy of high-intensity ion implantation and its simultaneous energy impact on the surface in accordance with the method described in [7].

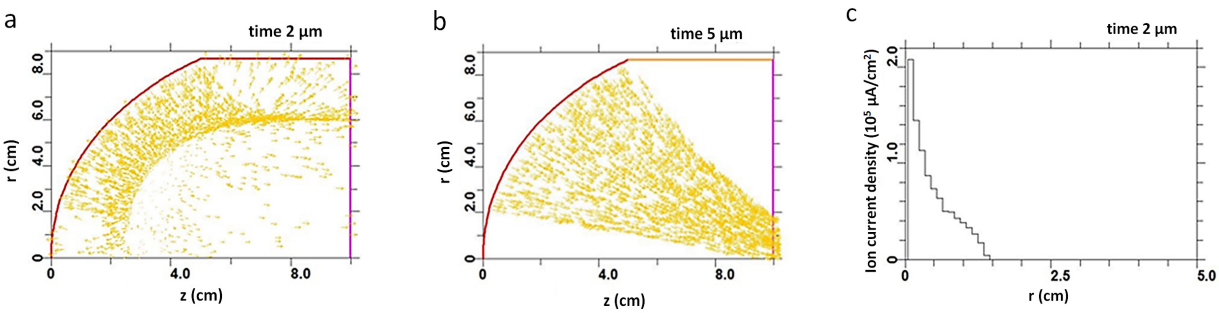


Fig.1. Portrait of an ion beam in drift space when ions with a beam current of 0.3 A are injected into vacuum at an ion energy of 10 keV (a), 30 keV (b) and the ion current density distribution in the system's geometric focus (c).

An increase in the injection current to 0.3 A and in the ion current density to $1.2 \cdot 10^{-3}$ A/cm$^2$ significantly changes the situation. As can be seen from Fig.1a, at an ion energy of 10 keV, the beam space charge effect leads to the appearance of a virtual anode and disruption of the efficient beam transport. When the ion energy increases to 30 keV, a virtual anode does not appear, the ion beam can be transported to the target (Fig.1b), but its focusing turns out to be poor due to the effect of the ion beam's own space charge (Fig.1c). The achievable maximum power density in the ion beam already exceeds 8 kW/cm$^2$.

## 4. Simulation of ion beam transport and focusing under conditions of space charge neutralization

Focusing should be improved by creating conditions for partial or complete ion beam space charge neutralization. In numerical simulation problems, one considers the case when during the ion beam injection in the drift space, there is plasma with a certain concentration, the residual gas ionization is taken into account and ion-electron emission occurs, or an additional electron source is used.

To study the possibility of achieving high power densities in the ion beam and taking into account the creation of various conditions for compensating its space charge, the numerical simulation was used to study the regularities of transport and focusing of the ion flow with an injection current of 1 A, corresponding to an initial current density of about $4 \cdot 10^{-3}$ A/cm$^2$. At an initial plasma density in the beam drift space of $10^{10}$ cm$^{-3}$, the injection of an ion beam with an energy of 10 keV gives the following results of numerical simulation. At the beginning of the injection pulse, the ions move radially and are well focused, as shown in Fig.2a. The potential distribution after 2 μs from the start of injection, shown in Fig.2b, demonstrates good beam space charge neutralization in the entire beam transport space. As follows from the calculation data presented in Fig.2c, at this time the beam is very well focused and at the focus the ion current density approaches 5 A/cm$^2$. This means that even at a low ion energy in this case it is possible to obtain a beam with a power density of about 50 kW/cm$^2$.

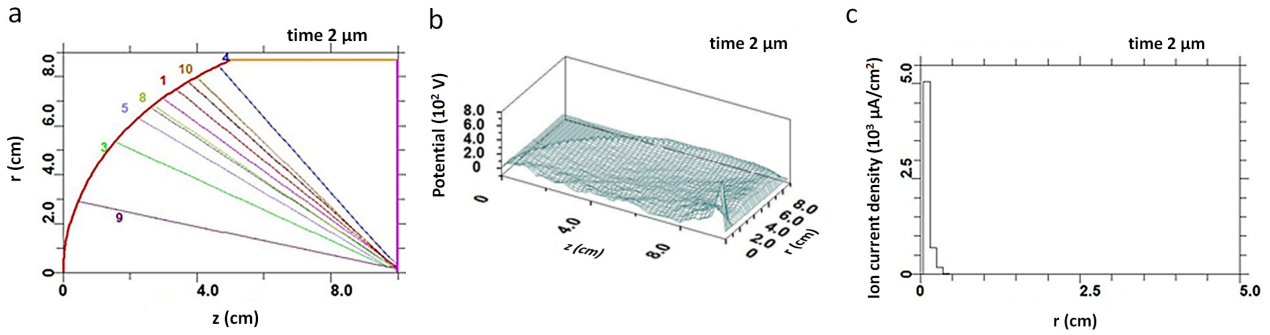


Fig.2. Ion trajectories on the second μs of beam injection (a), potential distribution in the beam drift space on 2 μs (b), ion current density distribution in the focal plane (c).

With an increase in the injection time, the conditions for high-intensity ion beam transport and focusing deteriorate dramatically. For example, the calculation results of the number of plasma electrons, plasma ions and beam ions at a point with coordinates $z = 4$ cm and $r = 4$ cm, presented in Fig.3a, show a rapid decrease in the density of ion and plasma electrons after the 2nd μs from the start of ion injection. After about 7 μs, the plasma ions are completely removed from the beam by its own electric field. Only plasma electrons are retained in the beam region, compensating its space charge. However, even at an initial plasma density of $10^{10}$ cm$^{-3}$, after the 10th μs, oscillations occur

and a virtual anode appears. The characteristic spatial distribution of the potential in this case takes the form shown in Fig.3b. As can be seen from the results of beam current simulation in the focal plane, its amplitude slowly decreases from the start of ion injection to approximately 10 μs. Then, due to the fact that electrons, heated up in oscillating electric fields, go to the walls, a virtual anode appears and the current rapidly decreases from 1 A to approximately 0.2A.

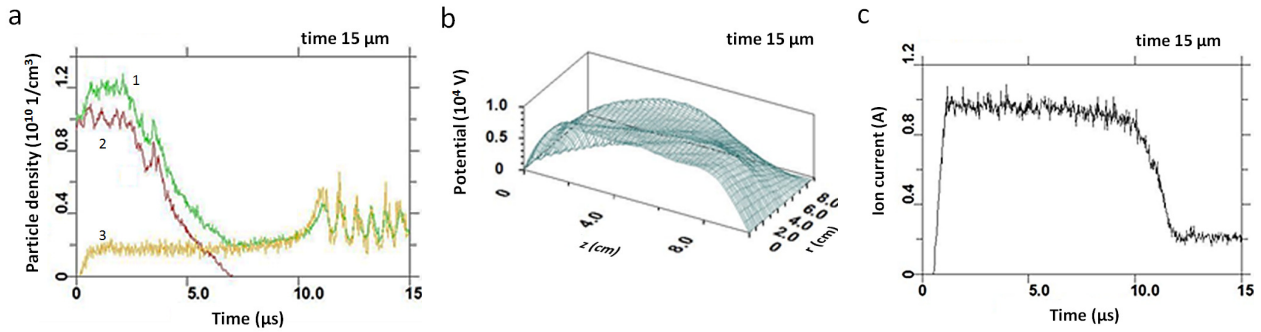


Fig.3. Change, depending on time, density of plasma electrons and ions and beam ions (a), potential distribution in space (b), dependence of the ion beam transported to the focal region on time (c). 1 – plasma electrons, 2 – plasma ions, 3 – beam's ion.

The situation can be slightly improved by taking into account the possibility of forming additional plasma due to the residual gas (nitrogen) ionization in the drift space by beam ions. In this case, as shown in Fig.4, after the first occurrence of the virtual anode, as in the previous case, the transported current amplitude sharply decreases. However, later on, during approximately 10 μs, due to the production of plasma electrons, the beam transport gradually improves. After 20 μs, there is a rapid increase in the ion current amplitude, which again leads to the appearance of a virtual anode. In the future, this process is periodically repeated. Figs.4b and 4c show the change in time of the total number of particles in the drift space and the density of plasma ions and electrons, as well as beam ions at a point in space with coordinates $z = 4$ cm and $r = 4$ cm.

A significant improvement in the conditions for ion beam transport was achieved when the generation of secondary electrons due to ion-electron emission from all surfaces was taken into account, in addition to the initial plasma in the drift space and taking into account the residual nitrogen ionization.

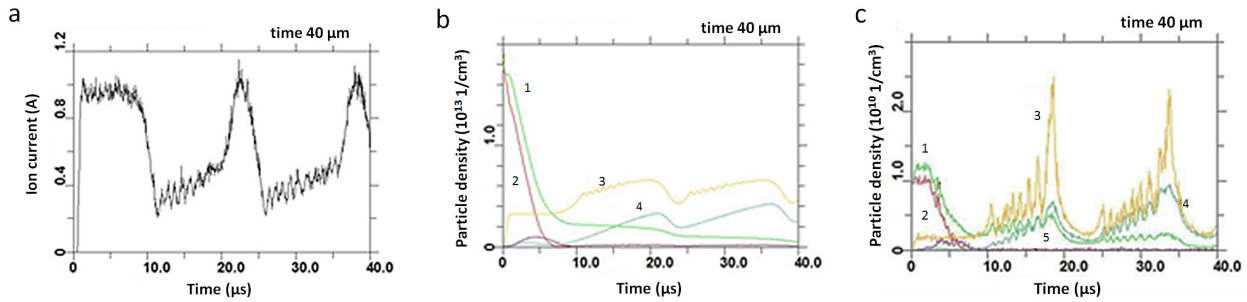


Fig.4. Dependence of the ion beam transported to the focal region on time (a), the total number of different particles in space (b), the dependence of the different particles' density at a point with coordinates $z = 4$ cm and $r = 4$ cm. 1 – plasma electrons, 2 – plasma ions, 3 – beam's ion, 4 – secondary electrons, 5 – electrons o ionized background gas (N).

Fig.5 represents the changes in the density of plasma ions and electrons, secondary electrons obtained due to ion-electron emission, electrons formed by residual nitrogen ionization and ion

beam density during 30 μs, at a point in space with coordinates $z = 4$ cm and $r = 4$, that demonstrate the absence of oscillations and the appearance of a virtual anode.

The potential distribution in the drift space shown in Fig.5b indicates satisfactory beam space charge compensation and the presence of a potential drop that does not exceed 1 kV. The possibility of increasing the ion current density on the collector to more than 3 A/cm$^2$ is demonstrated by the numerical simulation results presented in Fig.5c.

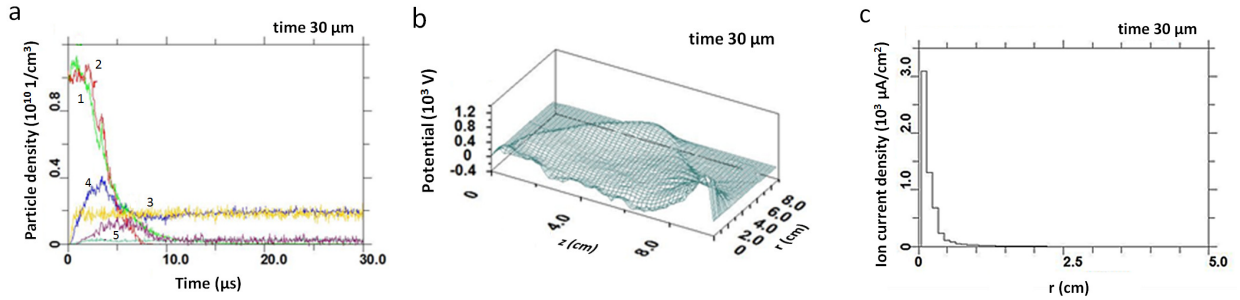


Fig.5. Time dependence of the density of plasma ions and electrons, secondary electrons obtained due to ion-electron emission, electrons formed by residual nitrogen ionization and ion beam density (a), potential distribution in drift space (b) and ion current density distribution on the collector (c). 1 – plasma electrons, 2 – plasma ions, 3 – beam's ion, 4 – secondary electrons, 5 – electrons o ionized background gas (N).

In further simulations, the ion energy was increased to 30 keV, and the injection current was maintained 1 A. Calculations showed that at an initial plasma density in the drift space of $3 \cdot 10^9$ cm$^{-3}$, plasma ions go to the walls in 7 μs (Fig.6a). Plasma electrons are heated up and also leave the ion beam. By 280 μs, the number of electrons decreases to the extent that a virtual anode is formed due to the beam space charge decompensation. A typical potential distribution at this time is shown in Fig.6b, and the beam's configuration portrait is shown in Fig.6c.

As in the case with ion energy of 10 keV, it was possible to improve the conditions for beam transport and focusing, when ion-electron emission was taken into account. Taking into account the increase in the ion energy, the ion beam focusing improved and, as a result, the maximum current density approached 5 A/cm$^2$. The maximum power density of the ion beam in this case reached 150 kW/cm$^2$.

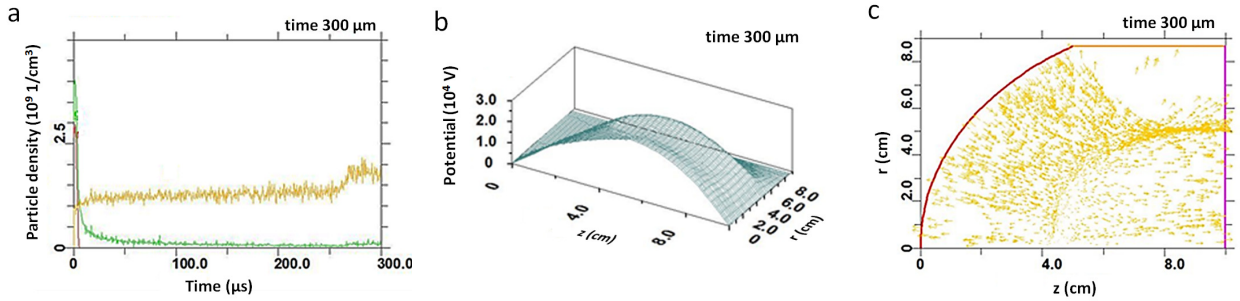


Fig.6. Dependence of the density of plasma ions and electrons, as well as beam ions on time (a), potential distribution (b) and beam's configuration portrait (c) at 300 μs when a virtual anode appears.

## 5. Conclusion

Numerical simulation of the features and regularities of metal ion beam formation from vacuum arc plasma with a power density of up to 150 kW/cm$^2$ was performed using the Karat code. The ballistic focusing of heavy ions has been studied at injection current from 0.1 to 1A and initial current density of up to 4 mA/cm$^2$. The article has studied the influence of the ion current density, accelerating voltage, and conditions for beam space charge neutralization on the high-power ion

beam's transport and focusing. The conditions for the virtual anode appearance have been determined and studied. It has been established that for long durations of ion beam formation at low pressures of the residual atmosphere, multiple appearance and disappearance of a virtual anode is possible.

**Acknowledgments**

This work was financially supported by the Russian Science Foundation (project No. 22-19-00051, https://rscf.ru/project/22-19-00051/).

**6. References**

[1] Poate J.M., Foti G., Jacobson D.C., *Surface Modification and Alloying by Laser, Ion, and Electron Beams,* (Berlin: Springer, 2013).
[2] Williams J.S., Poate J.M., *Ion Implantation and Beam Processing*. (Orlando: Academic, 1984).
[3] Anders A., *Handbook of Plasma Immersion Implantation and Deposition*. (New York: John Wiley & Sons, 2000).
[4] Ryabchikov A.I., *Surf. Coat. Technol.*, **388**, 125561, 2020; doi: 10.1016/j.surfcoat.2020.125561
[5] Ryabchikov A.I., Shevelev A.E., Sivin D.O., Ivanova A.I., Medvedev V.N., *Surf. Coat. Technol*., **355,** 123, 2018; doi: 10.1016/j.surfcoat.2018.02.111
[6] Koval N.N., Ryabchikov A.I., Sivin D.O., Akhmadeev Y.H., Ignatov D.Y., *Surf. Coat. Technol.*, **340**, 152, 2018; doi: 10.1016/j.surfcoat.2018.02.064
[7] Ryabchikov A.I., *IEEE Trans. Plasma Sci.*, **49**(9), 2529, 2021; doi: 10.1109/TPS.2021.3073942
[8] Tarakanov V.P., *User's Manual for CODE KARAT*. (Springfield: Berkley, Research Associates Inc., 1992).
[9] Ryabchikov A.I., Ananin P.S., Dektyarev S.V., Sivin D.O., Shevelev A.E., *Vacuum,* **143**, 447, 2017; doi: 10.1016/j.vacuum.2017.03.011